J. Fluid Mech. (2007), *vol.* 587, *pp.* 235–254.
doi:10.1017/S0022112007007355 Printed in the United Kingdom

Generation of solitary waves by transcritical flow over a step

R. H. J. GRIMSHAW[1], D.-H. ZHANG[2] AND K. W. CHOW[2]

[1]Department of Mathematical Sciences, Loughborough University, Loughborough, LE11 3TU, UK

[2]Department of Mechanical Engineering, University of Hong Kong, Pokfulam Road, Hong Kong

(Received 17 December 2006 and in revised form 18 May 2007)

It is well-known that transcritical flow over a localized obstacle generates upstream and downstream nonlinear wavetrains. The flow has been successfully modelled in the framework of the forced Korteweg–de Vries equation, where numerical and asymptotic analytical solutions have shown that the upstream and downstream nonlinear wavetrains have the structure of unsteady undular bores, connected by a locally steady solution over the obstacle, which is elevated on the upstream side and depressed on the downstream side. In this paper we consider the analogous transcritical flow over a step, primarily in the context of water waves. We use numerical and asymptotic analytical solutions of the forced Korteweg–de Vries equation, together with numerical solutions of the full Euler equations, to demonstrate that a positive step generates only an upstream-propagating undular bore, and a negative step generates only a downstream-propagating undular bore.

1. Introduction

The flow of a fluid over an obstacle is a classical and fundamental problem in fluid mechanics. Our concern here is with the upstream and downstream waves that may be generated. The most well-known scenario is free-surface flow, when the waves are water waves, but the same essential features arise in many other physical systems, such as the flow of a density-stratified fluid over topography when the relevant waves are internal waves. When the flow is not critical, that is, the imposed flow speed is not close to any linear long-wave speed, linear theory may be used to describe the wave field, and typically the full solution can be obtained using Fourier transforms, followed by classical phase- and group-velocity arguments (see, for instance, Lighthill 1978 and Whitham 1974). For instance, in the case of water waves, typically stationary lee waves are found downstream in subcritical flow (that is, the flow speed $U < c$, the linear long-wave speed), together with transients propagating both upstream and downstream, while only downstream-propagating transients are found in supercritical flow ($U > c$). However, these linear solutions fail near criticality ($U = c$), as then the wave energy cannot propagate away from the obstacle. In this case it is necessary to invoke weak nonlinearity to obtain a suitable theory, and it is now well established that the forced Korteweg–de Vries (fKdV) equation is an appropriate model.

For water waves on an undisturbed depth h, the fKdV equation is

$$-A_t - \Delta A_x + \mu A A_x + \lambda A_{xxx} + \frac{c}{2} F_x = 0, \tag{1.1}$$

where

$$\mu = \frac{3c}{2h}, \quad \lambda = \frac{ch^2}{6}, \quad c = (gh)^{1/2}. \tag{1.2}$$

Here $A(x,t)$ is the wave amplitude, here the surface elevation above the undisturbed depth h, while $F(x)$ is the obstacle profile and $\Delta = U - c$ is the criticality parameter ($\Delta < 0 (> 0)$ is the subcritical (supercritical) regime). The asymptotic regime where we expect equation (1.1) to hold can be characterized by a small parameter $\epsilon \ll 1$, where a balance between all terms holds for the scaling $F \sim \epsilon^4$, $A \sim \epsilon^2$, $\partial/\partial x \sim \epsilon$, $\partial/\partial t \sim \epsilon^3$, $\Delta \sim \epsilon^2$. The fKdV equation has been derived for water waves by Akylas (1984), Cole (1985), Mei (1986), Wu (1987), and Lee, Yates & Wu (1989), and for internal waves by Grimshaw & Smyth (1986) and Melville & Helfrich (1987) where the coefficients μ, λ and the speed c are then given by expressions involving the modal function for the relevant internal wave mode. Note that for water waves, the forcing provided by a bottom obstacle, or by an applied surface pressure field, or by a slender ship, are equivalent in the weakly nonlinear approximation. Numerical and aysmptotic analytical solutions of the fKdV equation by these and other authors have demonstrated that, for flow over a localized obstacle, in the transcritical regime the solution typically consists of upstream and downstream nonlinear wavetrains, connected by a locally steady solution over the obstacle which is elevated on the upstream side and depressed on the downstream side. These nonlinear wavetrains have the structure of unsteady undular bores. Near exact criticality, the upstream wavetrain is attached to the obstacle, and to a high degree of approximation consists of upstream-propagating solitary waves.

These theoretical predictions were anticipated in several laboratory experiments. For water waves the first reported observations of the upstream waves generated by a steadily moving ship were apparently made by Thews & Landweber (1934, 1935). Systematic experiments reported by Huang *et al.* (1982), Ertekin, Webster & Wehausen (1984) and Lee *et al.* (1989) established the presence of upstream-propagating solitary waves. As well as the numerical simulations of the fKdV equation, simulations of generalized Boussinesq equations by Wu & Wu (1982) and Lee *et al.* (1989), and of a Green–Naghdi model by Ertekin, Webster & Wehausen (1986) also confirmed the generation of upstream-propagating solitary waves by transcritical flow over an obstacle.

Zhang & Chwang (2001) simulated the full Euler equations for transcritical flow over an obstacle, and as well as confirming the basic scenario of the generation of upstream and downstream undular bores, found good agreement with the theory of Grimshaw & Smyth (1986) based on the fKdV equation. A particular feature of their numerical simulations was the exploration of the effect of the width of the obstacle, and in a limiting configuration they simulated transcritical flow over either a positive (forward-facing) step, or a negative (backward-facing) step. Their results showed that a positive step generates an upstream-propagating undular bore, and a negative step generates a downstream-propagating undular bore, thus suggesting that the upstream and downstream wavetrains generated by transcritical flow over a localized obstacle may be generated by separate processes. It is these simulations which have lead to the present investigation, where we seek an explanation for this behaviour in the framework of the fKdV equation (1.1), using both theoretical asymptotic solutions constructed using the techniques of Grimshaw & Smyth (1986) and numerical simulations.

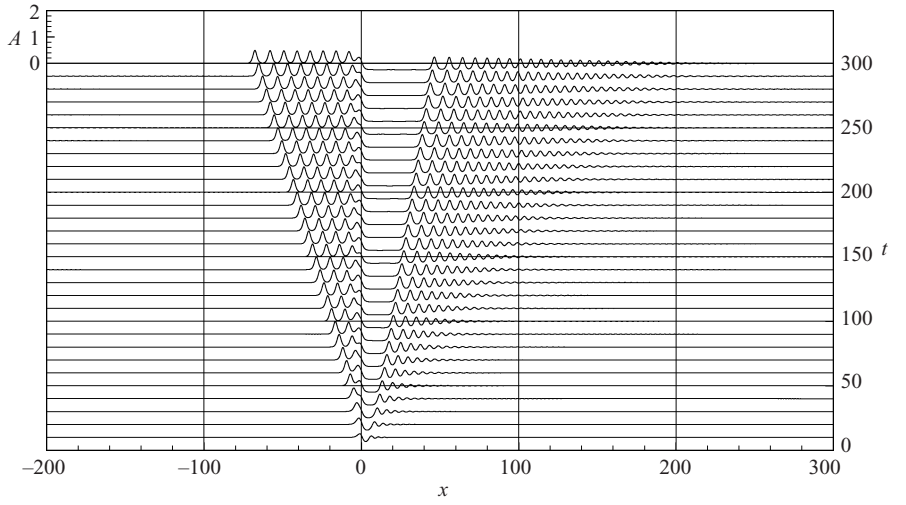

FIGURE 1. Numerical simulation of the fKdV equation (1.3) for localized forcing, with $F_M = 0.1$ and $\Delta = 0$. The forcing (not shown in the plot) is located at $x = 0$ and given by $F(x) = F_M \operatorname{sech}^2 x$.

In non-dimensional form, based on the velocity and length scales c, h equation (1.1) becomes

$$-A_t - \Delta A_x + \tfrac{3}{2} A A_x + \tfrac{1}{6} A_{xxx} + \tfrac{1}{2} F_x = 0. \tag{1.3}$$

Here the non-dimensional $\Delta = Fr - 1$ where $Fr = U/c$ is the Froude number. The fKdV equation in canonical form is obtained by putting

$$t^* = \tfrac{1}{6} t, \quad A^* = \tfrac{3}{2} A, \quad F^* = \tfrac{9}{2} F, \quad \Delta^* = 6\Delta. \tag{1.4}$$

Omitting the superscripts we obtain

$$-A_t - \Delta A_x + 6 A A_x + A_{xxx} + F_x(x) = 0. \tag{1.5}$$

This is to be solved with the initial condition that $A(x, 0) = 0$, which corresponds to the introduction of the topographic obstacle for $t \geqslant 0$. In a laboratory reference frame, this is equivalent to the situation in which the obstacle is at rest for $t < 0$ and is then moved at speed U to the left for $t > 0$. Our interest is the case when the forcing term represents a step, that is $F(x) = 0$ for $x < 0$ and then varies monotonically for $0 < x < W$ to a value $F_M > 0 (< 0)$ for $x > W$, corresponding to a positive (negative) step. In § 2 we construct asymptotic solutions in the spirit of Grimshaw & Smyth (1986), and in § 3 we describe some numerical simulations of the fKdV equation, and also of the full Euler equations for comparison.

2. Asymptotic solutions of the forced Korteweg–de Vries equation

2.1. *Critical flow over a localized obstacle*

Before considering the main case of interest, that is flow over a step, it is useful to present a summary of the theory for flow over a localized obstacle, based on Grimshaw & Smyth (1986) and Smyth (1987). First we recall the typical solutions of (1.3) when the forcing $F(x)$ is positive and localized. That is, $F(x)$ is positive, and non-zero only in a vicinity of $x = 0$, with a maximum value of $F_M > 0$. A numerical solution is shown in figure 1 for exact criticality. The solution is characterized by

upstream and downstream wavetrains connected by a locally steady solution over the obstacle. For subcritical flow ($\Delta < 0$) the upstream wavetrain weakens, and for sufficiently large $|\Delta|$ detaches from the obstacle, while the downstream wavetrain intensifies and for sufficiently large $|\Delta|$ forms a stationary lee wave field. On the other hand, for supercritical flow ($\Delta > 0$) the upstream wavetrain develops into well-separated solitary waves while the downstream wavetrain weakens and moves further downstream (for more details see Grimshaw & Smyth 1986 and Smyth 1987).

The origin of the upstream and downstream wavetrains can be found in the structure of the locally steady solution over the obstacle. Here we will use the canonical form (1.5) to describe the analysis; the analogous results for (1.3) are readily obtained from the scaling (1.4). In the transcritical regime this local steady solution is characterized by a transition from a constant state A_- upstream ($x < 0$) of the obstacle to a constant state A_+ downstream ($x > 0$) of the obstacle, where $A_- < 0$ and $A_+ > 0$. It is readily shown that $\Delta = 3(A_+ + A_-)$ independently of the details of the forcing term $F(x)$. Explicit determination of A_+ and A_- requires some knowledge of the forcing term $F(x)$. However, in the dispersionless, or 'hydraulic', limit when the linear dispersive term in (1.5) can be neglected, it is readily shown that, for all localized $F(x)$,

$$6A_\pm = \Delta \mp (12F_M)^{1/2}. \tag{2.1}$$

This expression also serves to define the transcritical regime, which is

$$|\Delta| < (12F_M)^{1/2}. \tag{2.2}$$

Thus upstream of the obstacle there is a transition from the zero state to A_-, while downstream the transition is from A_+ to 0; each transition is effectively generated at $x = 0$. Note that in the unscaled form (1.3) the regime (2.2) becomes $|\Delta| < (3F_M/2)^{1/2}$.

Both transitions are resolved by 'undular-bore' solutions as described in the Appendix (a typical undular bore is shown in figure 4). That in $x < 0$ is exactly described by (A 3) to (A 6) with x replaced by $\Delta t - x$, and A_0 by A_-. It occupies the zone

$$\Delta - 4A_- < \frac{x}{t} < \max\{0,\ \Delta + 6A_-\}. \tag{2.3}$$

Note that this upstream wavetrain is constrained to lie in $x < 0$, and hence is only fully realized if $\Delta < -6A_-$. Combining this criterion with (2.1) and (2.2) defines the regime

$$-(12F_M)^{1/2} < \Delta < -\tfrac{1}{2}(12F_M)^{1/2}, \tag{2.4}$$

where a fully developed undular bore solution can develop upstream. On the other hand, the regime $\Delta > -6A_-$ or

$$-\tfrac{1}{2}(12F_M)^{1/2} < \Delta < (12F_M)^{1/2} \tag{2.5}$$

is where the upstream undular bore is only partially formed, and is attached to the obstacle. In this case the modulus m of the Jacobian elliptic function varies from 1 at the leading edge (thus describing solitary waves) to a value m_- (< 1) at the obstacle, where m_- can be found from (A 5) by replacing x with Δt and A_0 with A_-.

The transition in $x > 0$ can also be described by (A 3) to (A 6) where we now replace x with $(\Delta + 6A_+)t - x$, A_0 with $-A_+$, and d with $d - A_+$. This 'undular bore' solution occupies the zone

$$\max\{0,\ \Delta - 2A_+\} < \frac{x}{t} < \Delta - 12A_+\,. \tag{2.6}$$

Here, this downstream wavetrain is constrained to lie in $x > 0$, and hence is only fully realized if $\Delta > 2A_+$. Combining this criterion with (2.1) and (2.2) defines the regime (2.5), and so a fully detached downstream undular bore coincides with the case when the upstream undular bore is attached to the obstacle. On the other hand, in the regime (2.4), when the upstream undular bore is detached from the obstacle, the downstream undular bore is attached to the obstacle, with a modulus $m_+(<1)$ at the obstacle, where m_+ can be found from (A 5) by replacing x with $\Delta - 6A_+$ and A_0 with A_+. Indeed a stationary lee wavetrain now develops just behind the obstacle (for further details, see Smyth 1987).

For the case when the obstacle has negative polarity (that is $F(x)$ is negative, and non-zero only in the vicinity of $x = 0$), the upstream and downstream solutions are qualitatively similar. However, the solution in the vicinity of the obstacle remains transient, and this causes a modulation of the 'undular bore' solutions.

2.2. *Critical flow over a step*

Here we consider positive and negative steps, where

$$\left.\begin{array}{ll} F(x) = 0 & \text{for} \quad x < 0, \\ F(x) = F_M & \text{for} \quad x > W, \end{array}\right\} \tag{2.7}$$

and $F(x)$ varies monotonically in $0 < x < W$. A positive (negative) step has $F_M > 0\,(<0)$. Strictly $F(x)$ should return to zero for some $L \gg W$. In this section we ignore this, and in effect assume that $L \to \infty$. In practice it means that the solutions constructed below are only valid for some limited time, determined by how long it takes for a disturbance to travel the distance L.

We shall sketch how the solution for the localized forcing described above becomes modified for a step. Adapting the approach used by Grimshaw & Smyth (1986) the first step is to construct the local steady-state solution, using the hydraulic limit. Thus, in the forcing region, $A = A(x), 0 < x < W$, while otherwise

$$A = A_- \quad \text{for} \quad x \to -\infty, \tag{2.8}$$

$$A = A_+ \quad \text{for} \quad x \to \infty. \tag{2.9}$$

Omitting the dispersive term in (1.5) it is readily found that

$$-\Delta A + 3A^2 + F = C, \tag{2.10}$$

or

$$6A = \Delta \pm (\Delta^2 + 12C - 12F)^{1/2}. \tag{2.11}$$

There are thus two branches. Application of the limits (2.8), (2.9) yields

$$C = -\Delta A_- + 3A_-^2 = -\Delta A_+ + 3A_+^2 + F_M,$$

giving a connection between A_- and A_+. The system is closed by determining the constant C from the long-time limit of the unsteady hydraulic solution, as in Grimshaw & Smyth (1986). That is, we omit the linear dispersive term in (1.5) and write the resulting nonlinear hyperbolic equation in the characteristic form

$$\frac{\mathrm{d}x}{\mathrm{d}t} = \Delta - 6A, \quad \frac{\mathrm{d}A}{\mathrm{d}t} = F_x(x), \tag{2.12}$$

This is then to be solved with the initial condition that $A = 0$ at $t = 0$. Note that these characteristic equations have the integral

$$-\Delta A + 3A^2 + F = F_0,$$

or

$$6A = \Delta \pm (\Delta^2 + 12F_0 - 12F)^{1/2},$$

where F_0 is the value of F at the initial time on each characteristic. There are again two branches, and the characteristic can switch branches at a turning point where $\mathrm{d}x/\mathrm{d}t = 0$ if there is a value of x where $\Delta^2 + 12F_0 = 12F$. At $t = 0$ we must choose the lower (upper) branch for $\Delta > 0\,(< 0)$.

Suppose first that the step is positive, $F_M > 0$. Then F_x is zero in $x < 0, x > W$ and $F_x > 0$ for $0 < x < W$. It follows that all characteristics have an initial slope Δ which then decreases. Then, for $\Delta \leqslant 0$, it is clear that all characteristics have a negative slope, and there are no turning points; in this case, clearly $A_+ = 0, C = F_M$ and the upper branch must be chosen in (2.11). Similarly, for $\Delta > (12F_M)^{1/2}$, it can be shown that there are no turning points, and all characteristics have a positive slope; in this case $A_- = 0, C = 0$ and the lower branch is chosen. But, for $0 < \Delta < (12F_M)^{1/2}$, all characteristics emerging from the step with $0 < 12F_0 < 12F_M - \Delta^2$ have a turning point and then go upstream into $x < 0$, while those with $12F_M - \Delta^2 < 12F_M < 0$ pass over the step and go downstream into $x > W$; it follows that $12C = 12F_M - \Delta^2$, and that $6A_+ = \Delta$, while A_- is then obtained from the upper branch of (2.11). In summary, the outcome is

$$\Delta \leqslant 0: \quad 6A_- = \Delta + (\Delta^2 + 12F_M)^{1/2}, \quad 6A_+ = 0, \tag{2.13}$$

$$0 < \Delta < (12F_M)^{1/2}: \quad 6A_- = \Delta + (12F_M)^{1/2}, \quad 6A_+ = \Delta, \tag{2.14}$$

$$\Delta > (12F_M)^{1/2}: \quad 6A_- = 0, \quad 6A_+ = \Delta - (\Delta^2 - 12F_M)^{1/2}. \tag{2.15}$$

In all cases, the upstream solution $A_- > 0$ is a 'shock' in the hydraulic limit (although in (2.15) the shock has zero strength and so can be ignored), which needs to be replaced with an 'undular bore' as in § 2.1. That is, the undular bore is again given by (A 3) to (A 6) with x replaced by $\Delta t - x$ and A_0 by A_-, so that

$$\Delta - \frac{x}{t} = 2A_- \left\{1 + m - \frac{2m(1-m)K(m)}{E(m) - (1-m)K(m)}\right\}$$

$$\text{for } \Delta - 4A_- < \frac{x}{t} < \max\{0, \Delta + 6A_-\}, \tag{2.16}$$

$$a = 2A_- m, \quad d = A_- \left\{m - 1 + \frac{2E(m)}{K(m)}\right\}. \tag{2.17}$$

Here A_- is given by (2.13), (2.14), (2.15), m is the modulus of the Jacobian elliptic function in (A 3), a is the wave amplitude, and d is the mean level (see (A 3), (A 4)) Note that in (2.17) we need to insert the extra requirement that this undular bore must be upstream of the step, and so lies in $x < 0$. For a fully detached undular bore, $\Delta + 6A_- < 0$, and combining this criterion with (2.13), (2.14), (2.15), we obtain the regime

$$\Delta < -2(F_M)^{1/2} < 0. \tag{2.18}$$

On the other hand the regime where $\Delta + 6A_- > 0$ but $\Delta - 4A_- < 0$, or

$$-2(F_M)^{1/2} < \Delta < (12F_M)^{1/2}, \tag{2.19}$$

is where the upstream undular bore is only partially formed and is attached to the obstacle. Note that the regimes (2.18), (2.19) for the unscaled equation (1.3) are $\Delta < -(F_M/2)^{1/2} < 0$ and $-(F_M/2)^{1/2} < \Delta < (3F_M/2)^{1/2}$ respectively.

Downstream, for $0 < \Delta < (12F_M)^{1/2}$ the hydraulic solution with $A_+ = \Delta > 0$ is terminated by a rarefraction wave, and so no undular-bore solution is needed. Instead

a weak oscillatory wavetrain is needed to smooth the corners. For $\Delta > (12F_M)^{1/2}$ (or $\Delta > (3F_M/2)^{1/2}$ in unscaled variables) there is no upstream disturbance, and again $A_+ > 0$ so that a rarefraction wave is needed.

Next consider the negative step, $F_M < 0$, for which the local steady state can be found in the hydraulic limit in a similar manner to that described above for a positive step. The outcome is

$$\Delta \geqslant 0 : \ 6A_- = 0, \ 6A_+ = \Delta - (\Delta^2 - 12F_M)^{1/2}, \tag{2.20}$$

$$-(-12F_M)^{1/2} < \Delta < 0 : \ 6A_- = \Delta, \ 6A_+ = \Delta - (-12F_M)^{1/2}, \tag{2.21}$$

$$\Delta < -(-12F_M)^{1/2} : \ 6A_- = \Delta + (\Delta^2 + 12F_M)^{1/2}, \ 6A_+ = 0. \tag{2.22}$$

Here the constant in (2.10) is $C = 0, -\Delta^2/12, F_M$ respectively. In all cases the downstream solution $A_+ < 0$ is a shock (in (2.22) the shock has zero strength), and needs to be replaced by an undular-bore solution. Now the undular bore is given by (A 3) to (A 6) with x replaced by $(\Delta + 6A_+)t - (x - W)$, A_0 by $-A_+$ and d by $d - A_+$. It occupies the zone

$$\max\{0, \ \Delta - 2A_+\} < \frac{x - W}{t} < \Delta - 12A_+, \tag{2.23}$$

where A_+ is given by (2.20), (2.21), (2.22), and we have inserted the requirement that the undular bore should lie downstream of the step in $x > W$. For a fully detached undular bore, $\Delta - 2A_+ > 0$, and combining with the criteria (2.20), (2.21), (2.22) we obtain the regime

$$\Delta > -(-3F_M)^{1/2}. \tag{2.24}$$

On the other hand, the regime where $\Delta - 2A_+ < 0$ but $\Delta - 12A_+ > 0$, or

$$-(-12F_M)^{1/2} < \Delta < -(-3F_M)^{1/2} < 0, \tag{2.25}$$

is where the undular bore is only partially formed. For $\Delta < -(-12F_M)^{1/2}$ we expect a stationary lee-wavetrain to form downstream. For the original unscaled equation (1.3) the regime (2.24), (2.25) becomes $\Delta > -(-3F_M/8)^{1/2}$ and $-(-3F_M/2)^{1/2} < \Delta < -(-3F_M/8)^{1/2}$ respectively.

For $\Delta < 0$ the upstream solution, $A_- < 0$, is terminated by a rarefraction wave and no shock is needed, but an oscillatory wavetrain is needed to smooth out the corners. For $\Delta > 0$ the upstream solution is zero.

2.3. *Steady solutions over a step*

The local steady solutions, described above in the hydraulic limit by (2.13), (2.14), (2.15) for $F_M > 0$ and by (2.20), (2.21), (2.22) for $F_M < 0$, are a subset of the full class of possible steady solutions. But, as noted above, they are the unique local steady solutions obtainable from the present initial condition ($A = 0$ at $t = 0$) in the hydraulic limit. Recently, Binder, Dias & Vanden-Broeck (2006) have given a comprehensive analytical and numerical analysis of the steady solutions for flow over an abrupt step, given by $F(x) = F_M H(x)$ (where $H(x)$ is the Heaviside function). Their work includes both the fully nonlinear regime and a weakly nonlinear analysis based on a steady forced KdV equation, and extends an earlier numerical study by King & Bloor (1987). Here, for completeness, we shall briefly review their work, and complement it by the analogous results using the hydraulic limit.

The steady solutions of (1.5) for $A = A(x)$ are given by

$$A_{xx} - \Delta A + 3A^2 + F = C. \tag{2.26}$$

In the hydraulic limit, the dispersive term A_{xx} is omitted, leading to (2.10), (2.11) as above. Let us first seek solutions such that $A \to A_\pm$ as $x \to \pm\infty$, that is upstream and downstream of the step respectively (see (2.8), (2.9)). Then $A_\pm$ are critical points of (2.26) and are given by

$$6A_+ = \Delta \pm (\Delta^2 + 12C - 12F_M)^{1/2}, \quad 6A_- = \Delta \pm (\Delta^2 + 12C)^{1/2}. \tag{2.27}$$

They exist for all allowed values of the constant C, that is $\Delta^2 + 12C > 12F_M$ for $F_M > 0$ and $\Delta^2 + 12C > 0$ for $F_M < 0$. In each case the upper branch is a centre, denoted by $A^c_\pm$, and the lower branch is a saddle point, denoted by $A^s_\pm$. Further, for $F_M > 0$, $A^c_- > A^c_+ > A^s_+ > A^s_-$, while for $F_M < 0$, $A^c_+ > A^c_- > A^s_- > A^s_+$. We also note that in the presence of a level $A_\pm$ the local criticality parameter is $\Delta_\pm = \Delta - 6A_\pm$, and hence a centre is always subcritical, while a saddle point is always supercritical. The task then is to determine how these critical points may be connected by an appropriate solution of (2.26) over the step.

Let us first consider the hydraulic limit, valid for a 'broad' step, when the connecting solution is described by (2.10), (2.11). Solutions exist for all allowed values of C, and describe either a centre to centre connection, or a saddle-point to saddle-point connection. Next, we recall that the locally steady solutions obtained above in § 2.2 for $F_M > 0$ are obtained by putting $12C = 12F_M, 12F_M - \Delta^2, 0$ for $\Delta \leqslant 0, 0 < \Delta < (12F_M)^{1/2}, \Delta > (12F_M)^{1/2}$ corresponding to (2.13), (2.14), (2.15) respectively; thus these represent a centre to centre connection, a centre to a double critical point (coincident centre and saddle point) connection, and a saddle-point to saddle-point connection respectively. For $F_M < 0$ the corresponding settings are $12C = 0, -\Delta^2, 12F_M$ for $\Delta \geqslant 0, -(-12F_M)^{1/2} < \Delta < 0, \Delta < -(-12F_M)^{1/2}$ corresponding to (2.20), (2.21), (2.22) respectively; thus these represent a saddle-point to saddle-point connection, a double critical point to a saddle-point connection, and a centre to centre connection respectively. Binder *et al.* (2006) confined their discussions to those cases where the steady solutions connected smoothly to the given upstream flow; that is, in our terminology, we seek solutions with $C = 0, A_- = 0$ in (2.26). As they note, there are then two branches for the downstream constant state A_+ (see (2.27)) for $C = 0$. For $F_M > 0$ these states exist only for $\Delta^2 > 12F_M$, but for $F_M < 0$ they exist for all Δ. They can be understood as bifurcations from the solutions $0, \Delta/3$ when $F_M = 0$, these representing a uniform undisturbed stream and the conjugate flow respectively. We note that these smooth connections are found for our present initial conditions only for $\Delta > (12F_M)^{1/2}$ when $F_M > 0$ (2.15), and for $\Delta > 0$ when $F_M < 0$ (2.20). In each case the connection from the zero state upstream is to that downstream state which has bifurcated from a uniform stream, rather than that which has bifurcated from the conjugate flow. Such solutions were found by King & Bloor (1987) and Binder *et al.* (2006) in their numerical calculations for fully nonlinear flow over an abrupt positive step (that is $F = F_M H(x)$, $F_M > 0$).

Next, we consider a 'narrow' step, represented by $F(x) = F_M H(x)$. This is the case studied by Binder *et al.* (2006), and we shall present a brief summary here. In this case (2.26) holds in $x < 0$ with $F = 0$, and in $x > 0$ with $F = F_M$; across $x = 0$ we require continuity of A, A_x. Thus, we have a steady KdV equation to solve in $x < 0, x > 0$, with the solutions to be matched at $x = 0$. The solutions can be constructed explicitly by quadrature, but as shown by Binder *et al.* (2006), it is more instructive to consider the solutions in the respective (A_x, A) phase planes, and note that at $x = 0$, one moves from an appropriate orbit in the upstream ($x < 0$) phase-plane to an appropriate orbit in the downstream ($x > 0$) phase-plane. Then, on imposing the limits $A \to A_\pm$ as $x \pm \infty$, we readily find that for all allowed values of the constant C, there are saddle-point

to saddle-point connections. That is, there are orbits connecting A^s_- to A^s_+; as above these are always supercritical, and $A^s_+ > (<) A^s_-$ according to whether $F_M > (<) 0$. However, unlike the 'broad' step case, there are no centre to centre connections; as we discuss below, these are replaced by connections between periodic orbits, representing waves. But, for certain special values of C we can find a connection between a saddle point and a centre, by the requirement that a centre for the upstream (downstream) phase-plane lies on the homoclinic orbit through the saddle point (that is, the solitary wave solution) for the downstream (upstream) phase-plane, according to whether $F_M > (<) 0$. Such solutions are 'hydraulic falls' in the terminology of Binder *et al.* (2006). They are given by $12C + \Delta^2 = 16F_M$ for $F_M > 0$, and by $12C + \Delta^2 = -4F_M$ for $F_M < 0$.

But, unlike the 'broad' step case where we can use the unsteady hydraulic solution (see (2.12)) to determine the value of C corresponding to the present initial condition that $A = 0$ at $t = 0$, in this 'narrow' step case it would seem that the determination of C requires the solution of the full unsteady fKdV equation (1.5). Hence, we are unable to make an explicit determination of C. Nevertheless, some guidance can be obtained by requiring that for sufficiently large $|\Delta|$ we expect that $A_- = 0$ when $\Delta > 0$ and $A_+ = 0$ for $\Delta < 0$. Thus, if we now require that $A_- = 0$, it follows that $C = 0$; this is the case discussed by Binder *et al.* (2006), as they required a smooth connection to the undisturbed upstream flow. For $\Delta > 0$, $A^s_- = 0$ is a saddle point (2.27), and there is a saddle-point to saddle-point connection to A^s_+; for $F_M > 0$ we need to have $\Delta > (12F_M)^{1/2}$, and for $F_M < 0$, it is sufficient that $\Delta > 0$. Indeed, this is precisely the same end result as in the 'broad' step case, see (2.15), (2.20) respectively. Also note that with $C = 0$ but $\Delta < 0$, the zero upstream state is now a centre, $A^c_- = 0$, and in general there are no connections to a uniform state downstream. Instead, as we discuss in the next paragraph, the connection is to periodic solutions describing waves. Next, let us suppose that $\Delta < 0$ and set $A_+ = 0$, so that $C = F_M$. But now A^c_+ is a centre, and in general, there are no connecting solutions to A_-. Again, we expect that the explanation here is that in this 'narrow' step case, the downstream steady solution may contain waves. Also note that with $C = F_M$ but $\Delta > 0$ the zero downstream state is a saddle point, $A^s_+ = 0$, and then although there is a saddle-point to saddle-point connection to A^s_-, it is not realized as an outcome of our 'broad' step unsteady analysis.

Finally, as discussed by Binder *et al.* (2006), this 'narrow' step case allows for connections to periodic orbits, representing the presence of uniform wavetrains, potentially both upstream and/or downstream. We emphasize that such uniform wavetrains are quite different from the unsteady undular bores we have constructed in § 2.2. To simplify the analysis, we shall consider here only the possibility that such uniform wavetrains occur downstream, and that the upstream condition is that $A \to A_-$ as $x \to -\infty$. First, suppose that $F_M > 0$, so that we require $12C + \Delta^2 > 12F_M$. Then as well as the saddle-point to saddle-point connections discussed above, there is a further senario: there is a connection from the uniform state A^c_- in all $x > 0$ to a periodic orbit surrounding the centre A^c_+ in all $x < 0$, provided that $12C + \Delta^2 \geqslant 16F_M$ where equality describes a 'hydraulic fall', as above. Next, suppose that $F_M < 0$, so that we require $12C + \Delta^2 > 0$. Now, as well as the saddle-point to saddle-point connections discussed above, there are two further scenarios: either there is a connection between the uniform state A^c_- in all $x < 0$ and a periodic orbit surrounding the centre A^c_+ in $x > 0$; or there is a connection between the saddle point A^s_- in $x < 0$ to a periodic orbit surrounding the centre A^c_+ in $x > 0$. Note that the 'hydraulic fall' solutions are not relevant here, as they are the limit of connections from upstream periodic orbits to a downstream centre, whereas here we are concerned with an upstream centre and a

downstream periodic orbit. The relevance of these wave solutions to the present study depends on the value of C, which for this 'narrow' step case is not known *a priori*.

Nevertheless, it is instructive to consider the values of C which yielded the 'broad' step outcomes (2.13), (2.14), (2.15) for $F_M > 0$, and (2.20), (2.21), (2.22) for $F_M < 0$ in § 2.2. Thus if $C = 0$, $F_M > 0$, $\Delta < -4(F_M)^{1/2}$, then there is a connection between the uniform state $A_-^c = 0$ in all $x < 0$ to a periodic orbit surrounding the centre $A_+^c < 0$ in all $x > 0$; the limiting solution at $\Delta = -4(F_M)^{1/2}$ has no waves, and is a 'hydraulic fall'. These allowed wavetrain solutions correspond to those found numerically by King & Bloor (1987) and Binder *et al.* (2006) for $F_M > 0$ in the full Euler equations. If $12C = 12F_M - \Delta^2$, $F_M > 0$ no wavetrain solutions are allowed, while if $C = F_M > 0$, $\Delta < -2(F_M)^{1/2}$, then there is a connection between the uniform state $A_-^c > 0$ in all $x < 0$ and a periodic orbit surrounding the centre $A_+^c = 0$ in all $x > 0$; the limiting solution at $\Delta = -2(F_M)^{1/2}$ is a 'hydraulic fall'. Otherwise, there are no such uniform wavetrain solutions.

Next, if $C = 0$, $F_M < 0$ there is a connection between the uniform state $A_-^c (= 0, \Delta/3$ according to whether $\Delta < 0, > 0)$ in all $x < 0$, and a periodic orbit surrounding the centre A_+^c in $x > 0$. In addition, there is a connection between the saddle point $A_+^s (= \Delta/3, 0$ according to whether $\Delta < 0, > 0)$ in $x < 0$ and a periodic orbit surrounding the centre A_+^c in $x > 0$. When the upstream state is zero, these allowed wavetrain solutions correspond to those found numerically by Binder *et al.* (2006) for $F_M < 0$ in the full Euler equations. If $12C = -\Delta^2$, $F_M < 0$ there are connections between the uniform state $A_- = \Delta/6$ (double critical point) and a periodic orbit around $A_+^c > A_-$ for all Δ, while if $C = F_M < 0$, $\Delta^2 < -12F_M$ there are connections between both the uniform state A_-^c, in all $x < 0$, and from the saddle point A_-^s, and a periodic orbit around the centre $A_+^c (= 0, \Delta/3$ according to whether $\Delta < 0, > 0)$ in all $x > 0$. Finally, we emphasize that our numerical solutions of the fKdV equation and of the full Euler equations (see § 3), for the present case of a zero initial condition, and for a 'broad' step, do not provide any evidence for the formation of steady uniform wavetrains downstream of the step, for either $F_M > 0$ or for $F_M < 0$.

3. Numerical results

3.1. *Numerical simulation of the forced Korteweg–de Vries equation*

The fKdV equation (1.3) is solved numerically by a finite difference scheme. We use a leapfrog scheme in time and central differencing in space,

$$\frac{\partial A}{\partial t} = \frac{A_i^{n+1} - A_i^{n-1}}{2\delta t} + O((\delta t)^2), \tag{3.1}$$

$$A\frac{\partial A}{\partial x} = \frac{1}{3}\left(A_{i+1}^n + A_i^n + A_{i-1}^n\right)\frac{A_{i+1}^n - A_{i-1}^n}{2\delta x} + O((\delta x)^2), \tag{3.2}$$

$$\frac{\partial^3 A}{\partial x^3} = \frac{A_{i+2}^n - 2A_{i+1}^n + 2A_{i-1}^n - A_{i-2}^n}{2(\delta x)^3} + O((\delta x)^2), \tag{3.3}$$

where we use a subscript to denote the spatial location and a superscript to denote the time level. Substituting these finite difference approximations back into the fKdV equation (1.3), we obtain an explicit scheme as follows:

$$A_i^{n+1} = A_i^{n-1} - \frac{\delta t}{\delta x}\left(\Delta - \frac{A_{i+1}^n + A_i^n + A_{i-1}^n}{2}\right)\left(A_{i+1}^n - A_{i-1}^n\right) + \frac{\delta t}{6(\delta x)^3}\left(A_{i+2}^n - 2A_{i+1}^n + 2A_{i-1}^n - A_{i-2}^n\right) + \delta t(F_x)_i^n. \tag{3.4}$$

The scheme (3.4) is second-order accurate in time and space, and is conditionally stable. Typical values used in our computations are $\delta t = 0.001$ and $\delta x = 0.1$. The forcing takes the form

$$F(x) = \frac{F_M}{2}(\tanh \gamma x - \tanh \gamma (x - L)), \tag{3.5}$$

where $F_M > 0$ is the height of the step (see (2.7)), L is the separation between the front and the rear steps, and $1/\gamma$ measures the width of the steps (i.e. a measure of W in (2.7)). Note that this form of forcing enables us to examine both a positive step at $x = 0$ and a negative step at $x = L$ in the same simulation, at least until the time it takes for a disturbance to travel a distance L across the step.

3.2. *Numerical simulation of the Euler equations*

The following summary is based on Zhang & Chwang (1999) reduced to the case of an inviscid fluid. The motion of an incompressible inviscid fluid under the influence of gravity is governed by the Euler equations and the equation of continuity, which in a body- and free-surface-fitted curvilinear coordinate system (ξ^i) have the form

$$\frac{\partial}{\partial t}\left(\frac{u_i}{J}\right) + \frac{\partial}{\partial \xi^j}\left(\frac{u_i}{J}\frac{\partial \xi^j}{\partial t} + \frac{u_i V^j}{J}\right) = -\frac{\partial}{\partial \xi^j}\left(\frac{\phi}{J}\frac{\partial \xi^j}{\partial x_i}\right), \tag{3.6}$$

$$\frac{\partial}{\partial \xi^j}\left(\frac{V^j}{J}\right) = 0, \tag{3.7}$$

where

$$J = \frac{\partial(\xi^1, \xi^2)}{\partial(x_1, x_2)}, \quad V^j = \frac{\partial \xi^j}{\partial x_k}u_k, \quad \phi = p + \frac{x_2}{Fr^2}. \tag{3.8}$$

Here x_i is a reference Cartesian coordinate system, u_i is the velocity component in the i-direction, p is the pressure, t is the time, J is the Jacobian of the transformation and V^j is the contravariant velocity component. The Euler equations are normalized by the undisturbed water depth h and the upstream velocity U. The pressure p is non-dimensionalized by ρU^2, time by h/U, the Froude number is defined here by $Fr = U/\sqrt{gh}$, and ρ is the constant density. Note that this non-dimensionalization differs from that used for the fKdV equation (1.5) where velocities were scaled by c, but the difference is small for transcritical flow. If $\eta(x_1, t)$ is the free-surface elevation, the kinematic condition is

$$\frac{\partial \eta}{\partial t} + u_1 \frac{\partial \eta}{\partial x_1} = u_2 \quad \text{at} \quad x_2 = \eta. \tag{3.9}$$

In the absence of surface tension, the dynamic condition on the free surface is

$$p = 0 \quad \text{at} \quad x_2 = \eta. \tag{3.10}$$

A slip boundary condition is imposed on the bottom, and a Neumann-type boundary condition is imposed at the downstream boundary.

These governing equations are discretized on a regular grid by a finite difference method. The velocity and pressure are evaluated at the computational cell centres. Spatial derivatives are discretized using a second-order central difference, and the QUICK scheme is used for discretization of the convection terms. Time marching is carried out using a time-splitting fractional step. It is a two-step predictor–corrector scheme. In the predictor step, an intermediate velocity field $\tilde{u}_i$ is computed explicitly by integrating equation (3.6) in time using the velocity and pressure from the previous time level n. Then the location of the free surface at the time level $n+1$ is evaluated by

	fKdV				Theory			
Δ	A_{w-}	A_-	A_{w+}	A_+	A_{w-}	A_-	A_{w+}	A_+
0.2	0.83	0.44	0.31	−0.16	0.80	0.40	0.32	−0.16
0.1	0.66	0.38	0.39	−0.20	0.66	0.33	0.40	−0.20
0.0	0.50	0.30	0.51	−0.26	0.52	0.26	0.52	−0.26
−0.1	0.39	0.22	0.64	−0.33	0.40	0.20	0.66	−0.33
−0.2	0.30	0.16	0.84	−0.40	0.32	0.16	0.80	−0.40
−0.3	0.24	0.13	0.64	−0.38	0.26	0.13	0.92	−0.46
−0.4	0.19	0.10	0.00	0.00	0.20	0.10	0.00	0.00
	fKdV				Euler			
Δ	A_{w-}	A_-	A_{w+}	A_+	A_{w-}	A_-	A_{w+}	A_+
0.2	0.83	0.44	0.31	−0.16	0.75	0.40	0.28	−0.18
0.1	0.66	0.38	0.39	−0.20	0.57	0.36	0.32	−0.21
0.0	0.50	0.30	0.51	−0.26	0.44	0.33	0.37	−0.25
−0.1	0.39	0.22	0.64	−0.33	0.32	0.20	0.43	−0.30
−0.2	0.30	0.16	0.84	−0.40	0.23	0.13	0.53	−0.36
−0.3	0.24	0.13	0.64	−0.38	0.16	0.08	0.57	−0.38
−0.4	0.19	0.10	0.00	0.00	0.10	0.01	0.00	0.00

TABLE 1. A quantitative comparison of the numerical simulations of the fKdV equation (1.3) and the Euler equations with the theory. $A_-(A_+)$ is the elevation just upstream (downstream) of the positive (negative) step at $x = 0(50)$ respectively, and $A_{w-}(A_{w+})$ is the amplitude of the leading wave in the corresponding undular bore.

integrating equation (3.9) explicitly, and the grid of the flow domain is re-generated to fit the newly determined free surface. Requiring the velocity field u_i^{n+1} to satisfy the continuity equation, a Poisson equation is obtained for solving the pressure increment $\delta\phi = \phi^{n+1} - \phi^n$, with the intermediate velocity field $\tilde{u}_i$ as the source term. The pressure field at the time level $n+1$ is then updated, and the velocity field u_i^{n+1} is obtained by modifying the intermediate velocity field $\tilde{u}_i$ using the pressure increment.

The solution domain in the vertical direction is of one unit length and 20 grid points are evenly distributed. In the horizontal direction, the solution domain is made sufficiently large so that the upstream wavetrain does not reach the upstream boundary at the final time of the computations. Thus, far upstream the flow is uniform and the free surface is undisturbed. Typically, 400 unit lengths are used and 600 grid points are distributed in the horizontal direction. The forcing is located in the middle of the solution domain ($x_1 = 0$). The grid is refined in the forcing region ($\delta x_1 \approx 0.5$) and gradually coarsened towards the two ends of the solution domain. The coarse grid in the region near the downstream boundary acts as a dissipation zone to prevent the reflection of waves into the solution domain. The time step is set to be $\delta t = 0.01$. The computation starts at the initial condition of zero velocity and a flat free surface.

3.3. *Description of results*

In figure 2(*a–c*) we show the simulations of the fKdV equation (1.3) for $F_M = 0.1$, $\gamma = 0.25$, $L = 50$ and $\Delta = 0.0, 0.2, -0.2$ respectively. The corresponding simulations for the Euler equations are shown in figure 3(*a–c*), and a quantitative comparison between our two sets of simulations and the theory described in § 2 is shown in table 1. In this table we compare the key features A_- (the upstream elevation at the step at $x = 0$), A_+ (the downstream depression at the step at $x = 50$), A_{w-} (the amplitude of the leading wave upstream) and A_{w-} (the amplitude of the leading

wave downstream). Note that in the present theory $A_{w-} = 2A_-$ and $A_{w+} = -2A_+$ (see the Appendix). It is important to note here that the numerical results are for the non-dimensional but unscaled fKdV equation (1.3) rather than for the canonical form (1.5) for which the theory was developed. The connection between them is described by (1.4) and in particular it follows that the numerical values corresponding to (1.5) are $F_M^* = 0.45$, $\Delta^* = 0, 0, 1.2, -1.2$

First we consider the results for the fKdV equation. When $\Delta = 0$ (figure 2*a*) we see that an upstream undular bore is attached to the positive step at $x = 0$, and a downstream undular bore propagates away from the negative step at $x = 50$, leaving a depression zone behind. Further, there is no evidence of a disturbance generated over the step. This scenario is in complete accord with our theoretical predictions. A quantitative comparison is displayed in table 1 where we see that there is excellent agreement. The largest discrepancy is for A_- upstream, which is the hardest quantity to estimate from the numerical solution as the upstream undular bore is attached to the step at $x = 0$. In this case of exact resonance the hydraulic limit predicts that the entire solution outside the step is exactly the same as that for flow over a localized positive forcing; indeed we see that $A_- = (12F_M)^{1/2}$ (see (2.13)) for a positive step and $A_+ = -(12F_M)^{1/2}$ (see (2.20)) for a negative step, which are exactly the same values of $A_\pm$ as predicted by (2.1) for a localized obstacle. In this case the hydraulic limit predicts that there is no communication between the two ends of the step. Small-amplitude dispersive waves, in the fKdV equation (1.3) have a phase speed $c = \Delta + k^2/6$ and a group velocity of $c_g = \Delta + k^2/2$, where k is the wavenumber. Such waves are not within the scope of the hydraulic limit, but may be generated as transients. With $\Delta = 0$ as here, if present they can only propagate downstream. However, we see from figure 2(*a*) that if such waves were generated, they must have very small amplitudes as they cannot be detected above the noise level in figure 2(*a*). Further, we note that the discussion of the allowed steady solutions in § 2.3 did not reveal the presence of uniform wavetrains downstream of the positive step (at $x = 0$) for this parameter setting. Also, although this analysis did allow for such uniform wavetrains downstream of the negative step (at $x = L$), they were not detected in our numerical simulations.

Next, for the supercritical case (figure 2*b*) we see there is again an upstream undular bore attached to the positive step at $x = 0$, and a downstream undular bore propagating away from the negative step at $x = 50$, leaving a depression zone behind. But now there is a positive rarefraction wave generated over the step, emanating from $x = 0$. Again, this scenario is in complete accord with our theoretical predictions. After taking account of the scalings (1.4) the parameter values for figure 2(*b*) place the upstream solution in the regime (2.19) for an attached undular bore, here $-0.22 < \Delta < 0.39$, and the downstream solution in the regime (2.24) for a fully detached undular bore, here $\Delta > -0.19$. From table 1 we see that there is again good agreement with the theoretical predictions, with the largest discrepancy again being for A_-. In this supercritical case, while the upstream and downstream solutions have the same qualitative structure as that for flow over a localized obstacle, the predicted values of $A_\mp$ are different. The scenario described above and depicted in figure 2(*b*) persists until the rarefraction wave reaches the end of the step at $x = 50$; since the leading edge of this rarefraction wave propagates with a speed Δ, this will occur when $t \approx L/\Delta = 250$. After this time, there will be an adjustment to the whole solution which will eventually settle down to the same solution as that described by Grimshaw & Smyth (1986) for flow over a localized obstacle. As for the critical case, we cannot detect the presence of any transient small-amplitude dispersive waves,

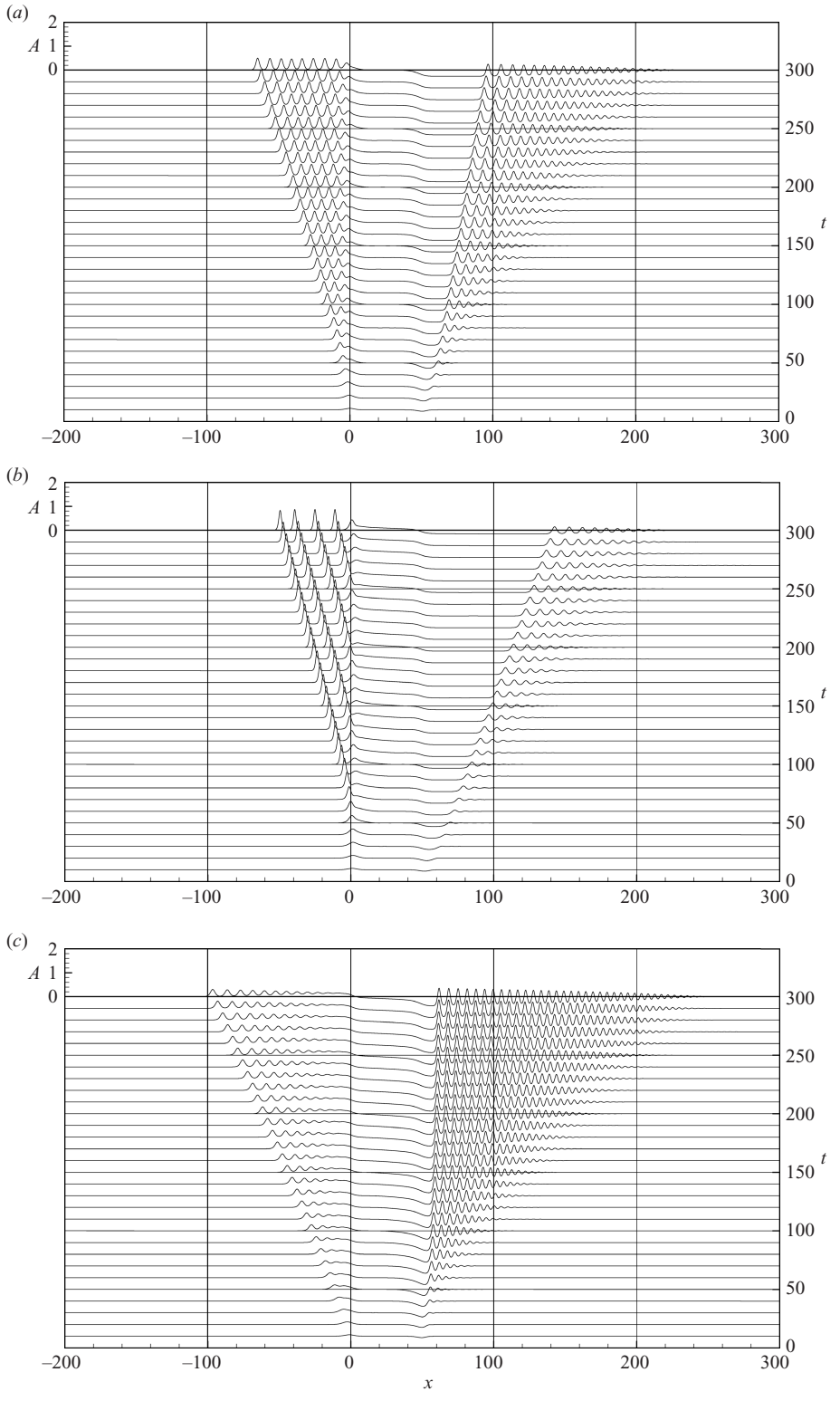

FIGURE 2. Numerical simulation of the fKdV equation (1.3) for the forcing (3.5), with $F_M = 0.1$, $\gamma = 0.25$, $L = 50$, and (*a*), $\Delta = 0$, (*b*) $\Delta = 0.2$, (*c*) $\Delta = -0.2$.

which if present must propagate downstream. Again we note that the discussion of the allowed steady solutions in § 2.3 did not reveal the presence of uniform wavetrains downstream of the positive step for this parameter setting, but did allow for the possibility of such uniform wavetrains downstream of the negative step, although these were not detected in our numerical simulations.

For the subcritical case (figure 2*c*) there is now a fully detached upstream bore, while the downstream bore has intensified and propagates more slowly, but is still fully detached. There is a negative rarefraction wave propagating upstream, emanating from $x = 50$. Again, this scenario is in accord with our theoretical predictions. But we note that the parameter values of figure 2(*c*) would place the upstream solution in the regime (2.19), here $-0.22 < \Delta < 0.39$, for an attached undular bore, and the downstream solution in regime (2.25) (here $-0.38 < \Delta < -0.19$) also for an attached undular bore. However, our numerical results for $\Delta = -0.2$ apparently place the upstream solution in the regime (2.18), here $\Delta < -0.22$, for a detached undular bore, and the downstream solution in the regime (2.24), here $\Delta > -0.19$, again for a detached undular bore. But because the value of Δ is very close to the boundaries of these regimes, we attribute this small discrepancy to errors in estimating $A_{\mp}$, and hence the regime boundaries, from the hydraulic limit. Nevertheless there is good quantitative agreement with our theoretical predictions, see table 1. As for the supercritical case, although the upstream and downstream solutions have the same qualitative structure as that for flow over a localized obstacle, the quantitative values of $A_{\mp}$ are different. But again, the scenario described above and depicted in figure 2(*c*) will only persist until the rarefraction wave reaches the end of the step at $x = 0$; since the leading edge of this rarefraction wave propagates with a speed $-\Delta$, this will occur when $t \approx L/\Delta = 250$. After this time, there will be an adjustment to the whole solution which will eventually settle down to the same solution as that described by Grimshaw & Smyth (1986) for flow over a localized obstacle. Again, as for the previous two cases, we cannot detect the presence of any transient small-amplitude dispersive waves, although in this subcritical case they can propagate upstream for wavenumbers $k < \sqrt{2|\Delta|}$ (note that the most likely wavenumber to be generated is $k \sim \gamma$ which for our parameter setting implies upstream propagation). In this case the discussion of the allowed steady solutions in § 2.3 indicates that a uniform wavetrain downstream of the positive step may arise from a zero state upstream if $\Delta < -0.45$, or from a uniform positive state upstream if $\Delta < -0.22$, but is not allowed for our parameter setting of $\Delta = -0.2$. But numerical simulations with $\Delta = -0.3, -0.4$ also failed to find such uniform wavetrains. Although the steady analysis of § 2.3 did allow for the possibility of uniform wavetrains downstream of the negative step, they again were not detected in our numerical simulations.

The corresponding results for the Euler equations are shown in figure 3(*a–c*). We see that there is always a good qualitative agreement, but as shown in table 1, the quantitative results are different. The amplitudes of the leading upstream and downstream waves, and the amplitudes of the upstream elevation and the downstream depression are consistently smaller than the corresponding entries for the fKdV equation. We attribute this to the effect of nonlinearity, as when the forcing amplitude F_M is reduced from 0.1 to 0.05, we find that the quantitative agreement is significantly improved. In this context we note that a similar discrepancy was found by Zhang & Chwang (2001) for the waves produced by flow over a localized obstacle. This discrepancy in the amplitudes also accounts for the different locations and speeds of the waves when comparing the fKdV simulations with the Euler equation simulations. Nevertheless, we can note that, importantly, the variation of all the

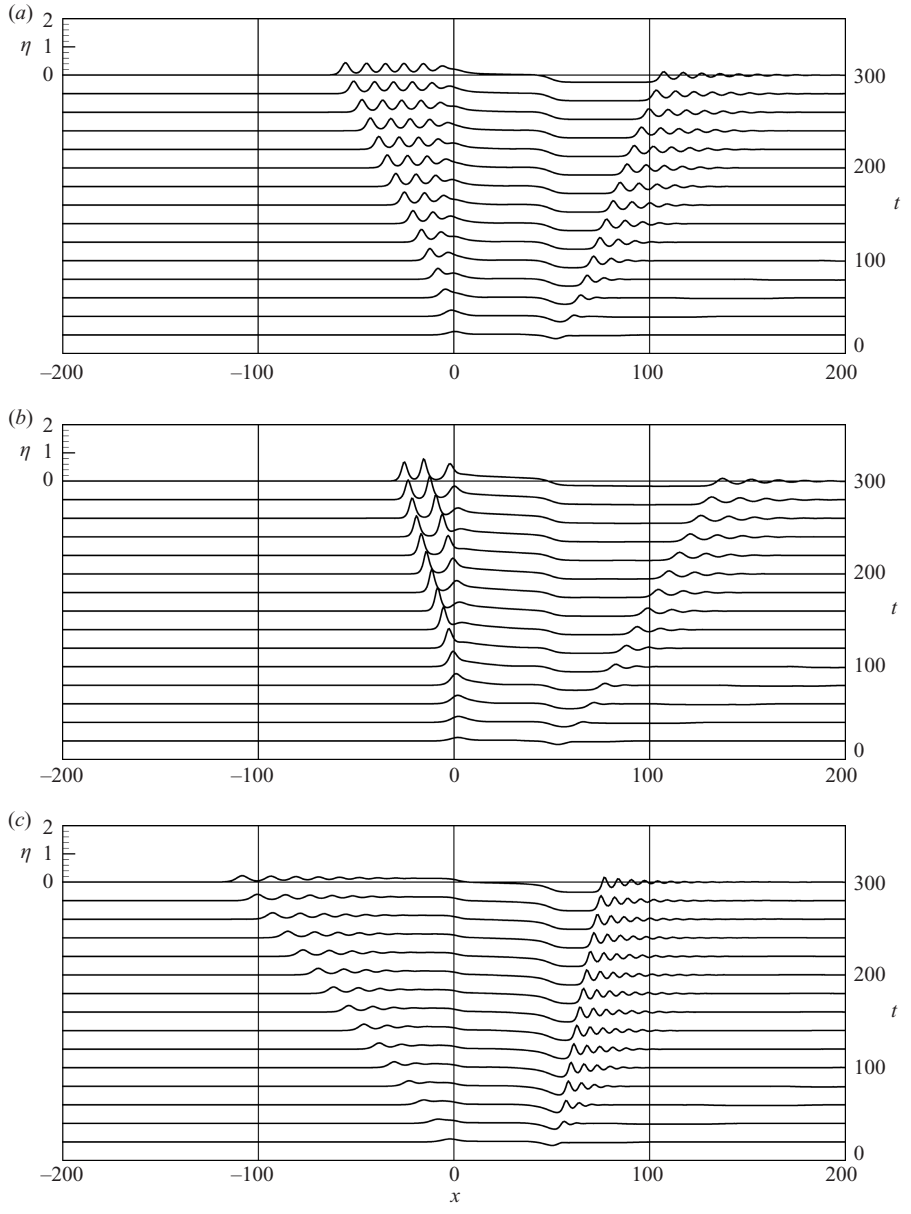

FIGURE 3. Numerical simulation of the Euler equations for the forcing (3.5), with $F_M = 0.1$, $\gamma = 0.25$, $L = 50$, and (*a*) $\Delta = 0$, (*b*) $\Delta = 0.2$, (*c*) $\Delta = -0.2$.

predicted amplitudes and elevations as Δ is varied follow the same trend for both the fKdV and Euler equations. Further, in all the Euler equation cases we simulated there was no evidence of any other wavetrains generated than those predicted by the fKdV equation. In particular, over the step itself, the only wave generated is a downstream- (upstream-) propagating rarefraction wave for $\Delta > 0 (< 0)$, just as in the fKdV equation. We infer, at least for the small-amplitude steps we have considered here, that the fKdV equation with its upstream and downstream undular bores provides a very good guide for transcritical flow over a step.

4. Conclusions

In this paper, we have explored transcritical flow over a step primarily in the framework of the forced Korteweg–de Vries (fKdV) equation (1.5), using both asymptotic analysis and numerical simulations. Our results show that a positive step generates an upstream-propagating undular bore formed by a (stationary) elevation upstream of the step, and a negative step generates a downstream-propagating undular bore formed by a (stationary) depression downstream of the step. The extent and strengths of the undular bores vary with the criticality parameter Δ. Although our emphasis here has been on water waves, our results apply in many other physical contexts as the fKdV equation is a canonical model for transcritical flow past an obstacle. In the water wave context, direct simulations of the full Euler equations confirm the scenarios identifed here in the fKdV model, provided of course that the obstacle, and hence the waves generated, have sufficiently small amplitudes.

All the numerical results displayed here have been obtained for the obstacle (3.5) with $F_M > 0$, that is, the flow encounters first a positive step, followed by a long constant height section, which is then terminated by a negative step. However, the analogous results when $F_M < 0$ in (3.5), that is, the flow encounters first a negative step, then a long constant height section terminated by a positive step, can be inferred from the results we have obtained. Thus, as discussed by Zhang & Chwang (2001), we would expect to see a depression and a downstream-propagating undular bore form at the negative step, and an elevation and an upstream-propagating undular bore form at the positive step. But, unlike the case for $F_M > 0$, with $F_M < 0$ these undular bores will meet and interact over the step itself. Although an analysis of this interaction may be possible in the framework of the Whitham equations (see the Appendix), we shall not attempt this quite daunting task. Instead we note that numerical simulations of the fKdV equation for a negative obstacle by Grimshaw & Smyth (1986) and others, and the numerical simulations of the Euler equations by Zhang & Chwang (2001) indicate that the outcome of this interaction is again upstream-propagating and downstream-propagating undular bores, but the solution over the obstacle or step remains unsteady.

Finally, we have already noted that the long-time solution for flow over a step of finite length (that is, (3.5) for instance with $F_M > 0, \gamma L \gg 1$) will be that predicted by Grimshaw & Smyth (1986) in the framework of the fKdV equation for flow over a localized obstacle. Indeed, at exact criticality Δ, the wavetrains generated by the elongated step are in fact exactly the same as those predicted for flow over a localized obstacle. Otherwise, for $\Delta \neq 0$, the upstream and downstream undular bores initially generated by the positive and negative steps have (slightly) different amplitudes to those generated by a localized obstacle, but for sufficiently long times ($t > L/|\Delta|$ there is communication between the two steps by a rarefraction wave, followed by an adjustment to precisely the same solution as predicted by Grimshaw & Smyth (1986).

Partial financial support for this work was provided by the Research Grants Council of Hong Kong through contracts HKU 7123/05E.

Appendix. Undular bore

The term 'undular bore' is widely used in the literature in a variety of contexts and has several different meanings. Here, we need to make it clear that we are concerned with non-dissipative flows, in which case an undular bore is intrinsically unsteady. In general, an undular bore is an oscillatory transition between two different basic

states. A simple representation of an undular bore can be obtained from the solution of the KdV equation

$$A_t + 6AA_x + A_{xxx} = 0, \tag{A 1}$$

with the initial condition that

$$A = A_0 H(-x), \tag{A 2}$$

where we assume at first that $A_0 > 0$. Here $H(x)$ is the Heaviside function (i.e. $H(x) = 1$ if $x > 0$ and $H(x) = 0$ if $x < 0$). The solution can in principle be obtained through the inverse scattering transform. However, it is more instructive to use the asymptotic method developed by Gurevich & Pitaevskii (1974) and Whitham (1974). In this approach, the solution of (A 1) with this initial condition is represented as the modulated periodic wavetrain

$$A = a\{b(m) + \mathrm{cn}^2(\kappa(x - Vt); m)\} + d, \tag{A 3}$$

where

$$b = \frac{1-m}{m} - \frac{E(m)}{mK(m)}, \quad a = 2m\kappa^2,$$

and

$$V = 6d + 2a\left\{\frac{2-m}{m} - \frac{3E(m)}{mK(m)}\right\}. \tag{A 4}$$

Here $\mathrm{cn}(x; m)$ is the Jacobian elliptic function of modulus m and $K(m)$, $E(m)$ are the elliptic integrals of the first and second kind respectively $(0 < m < 1)$, a is the wave amplitude, d is the mean level, and V is the wave speed. The spatial period is $2K(m)/\kappa$. This family of solutions contains three free parameters, which are chosen from the set (a, κ, V, d, m). As $m \to 1$, $\mathrm{cn}(x|m) \to \mathrm{sech}(x)$ and then the cnoidal wave (A 3) becomes a solitary wave, riding on a background level d. On the other hand, as $m \to 0$, $\mathrm{cn}(x|m) \to \cos x$ and so the cnoidal wave (A 3) collapses to a linear sinusoidal wave (note that in this limit $a \to 0$).

The asymptotic method of Gurevich & Pitaevskii (1974) and Whitham (1974) is to let expression (A 3) describe a modulated periodic wavetrain in which the amplitude a, the mean level d, the speed V and the wavenumber κ are all slowly varying functions of x and t. The outcome is a set of three nonlinear hyperbolic equations for three of the available free parameters, chosen from the set (a, κ, V, d, m), or rather better, from an appropriate combinations of them. These equations are often called the Whitham equations. The relevant asymptotic solution corresponding to the initial condition (A 2) is then constructed in terms of the similarity variable x/t, and is given by

$$\frac{x}{t} = 2A_0\left\{1 + m - \frac{2m(1-m)K(m)}{E(m) - (1-m)K(m)}\right\} \quad \text{for} \quad -6A_0 < \frac{x}{t} < 4A_0, \tag{A 5}$$

$$a = 2A_0 m, \quad d = A_0\left\{m - 1 + \frac{2E(m)}{K(m)}\right\}. \tag{A 6}$$

A plot of this expression is shown in Figure 4. Ahead of the wavetrain where $x/t > 4A_0$, $A = 0$ and at this end, $m \to 1$, $a \to 2A_0$ and $d \to 0$; the leading wave is a solitary wave of amplitude $2A_0$ relative to a mean level of 0. Behind the wavetrain where $x/t < -6A_0$, $A = A_0$ and at this end $m \to 0$, $a \to 0$, and $d \to A_0$; the wavetrain is now sinusoidal with a wavenumber κ given by $\kappa^2 = A_0$ (this holds throughout the wavetrain, so all waves have the same spatial wavelength). Further, it can be shown

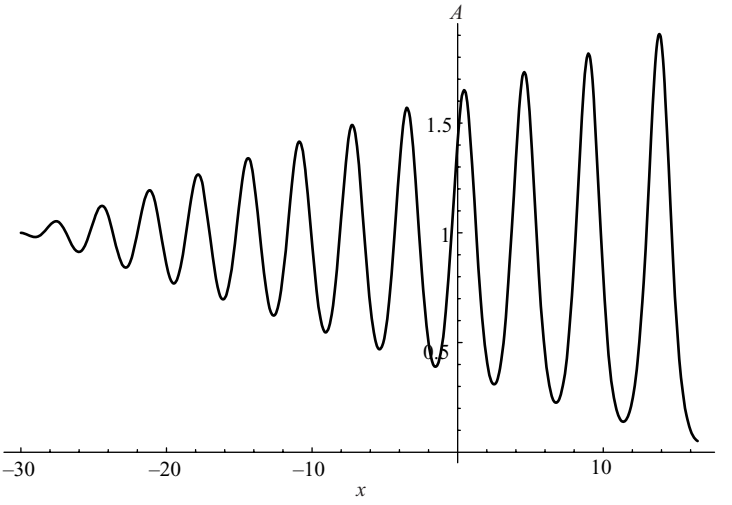

FIGURE 4. A plot of the undular bore given by (A 5), (A 6) for $A_0 = 1$, $t = 5$.

that on any individual crest in the wavetrain, $m \to 1$ as $t \to \infty$. In this sense, the undular bore evolves into a train of solitary waves.

If $A_0 < 0$ in the initial condition (A 3), then an 'undular bore' solution analogous to that described by (A 3), (A 5) does not exist. Instead, the asymptotic solution is a rarefraction wave,

$$\begin{aligned} A &= 0 \quad \text{for} \quad x > 0, \\ A &= \frac{x}{6t} \quad \text{for} \quad A_0 < \frac{x}{6t} < 0, \\ A &= A_0 \quad \text{for} \quad \frac{x}{6t} < A_0 (< 0). \end{aligned}$$

Small oscillatory wavetrains are needed to smooth out the discontinuities in A_x at $x = 0$ and $x = -6A_0$, see Gurevich & Pitaevskii (1974).

REFERENCES

AKYLAS, T. R. 1984 On the excitation of long nonlinear water waves by moving pressure distribution. *J. Fluid Mech.* **141**, 455–466.

BINDER, B. J., DIAS, F. & VANDEN-BROECK, J.-M. 2006 Steady free-surface flow past an uneven channel bottom. *Theor. Comput. Fluid Dyn.* **20**, 125–144.

COLE, S. L. 1985 Transient waves produced by flow past a bump. *Wave Motion* **7**, 579–587.

ERTEKIN, R. C., WEBSTER, W. C. & WEHAUSEN, J. V. 1984 Ship generated solitons. *Proc. 15th Symp. Naval Hydrodyn., Hamburg*, pp. 347–364.

ERTEKIN, R. C., WEBSTER, W. C. & WEHAUSEN, J. V. 1986 Waves caused by a moving disturbance in a shallow channel of finite width. *J. Fluid Mech.* **169**, 275–292.

GRIMSHAW, R. H. J. & SMYTH, N. F. 1986 Resonant flow of a stratified fluid over topography. *J. Fluid Mech.* **169**, 429–464.

GUREVICH, A. V. & PITAEVSKII, L. P. 1974 Nonstationary structure of a collisionless shock wave. *Sov. Phys. JETP* **38**, 291–297.

HUANG, D. B., SIBUL, O. J., WEBSTER, W. C., WEHAUSEN, J. V., WU, D. M. & WU, T. Y. 1982 Ships moving in the transcritical range. *Proc. Conf. on Behaviour of Ships in Restricted Waters, Varna, Bulgaria*, pp. 26-1–26-10.

KING, A. C. & BLOOR, M. I. G. 1987 Free-surface flow over a step. *J. Fluid Mech.* **182**, 193–208.

Lee, S. J. Yates, G. T. & Wu, T. Y. 1989 Experiments and analyses of upstream-advancing solitary waves generated by moving disturbances. *J. Fluid Mech.* **199**, 569–593.

Lighthill, J. 1978 *Waves in Fluids.* Cambridge University Press.

Mei, C. C. 1986 Radiation of solitons by slender bodies advancing in a shallow channel. *J. Fluid Mech.* **162**, 53–67.

Melville, W. K. & Helfrich, K. R. 1987 Transcritical two-layer flow over topography. *J.Fluid Mech.* **178**, 31–52.

Smyth, N. F. 1987 Modulation theory for resonant flow over topography. *Proc. R. Soc. Lond.* A **409**, 79–97.

Thews, J. G. & Landweber, L. 1934 The influence of shallow water on the resistance of a cruiser model. *US Experimental Model Basin, Washington, D.C.*, Rep. 408.

Thews, J. G. & Landweber, L. 1935 A thirty-inch model of the S.S. Clairton in shallow water. *US Experimental Model Basin, Washington, D.C.*, Rep. 414.

Whitham, G. B. 1974 *Linear and Nonlinear Waves.* Wiley.

Wu, T. Y. 1987 Generation of upstream advancing solitons by moving disturbances. *J. Fluid Mech.* **184**, 75–99.

Wu, D. M. & Wu, T. Y. 1982 Three-dimensional nonlinear long waves due to moving surface pressure. *Proc. 14th Symp. Naval Hydrodyn., Washington*, pp. 103–129.

Zhang, D.-H. & Chwang, A. T. 1999 On solitary waves forced by underwater moving objects. *J. Fluid Mech.* **389**, 119–135.

Zhang, D.-H. & Chwang, A. T. 2001 Generation of solitary waves by forward- and backward-step bottom forcing. *J. Fluid Mech.* **432**, 341–350.